Experimental Techniques (2022) 46:249–256
https://doi.org/10.1007/s40799-021-00478-w

RESEARCH PAPER

Fault Diagnosis of Rolling Bearing Based on Fractional Fourier Instantaneous Spectrum

J-h. Cai [1] · Y-l. Xiao [2] · L-y. Fu [1]

Received: 28 September 2020 / Accepted: 20 April 2021 / Published online: 5 May 2021

Abstract

Fractional Fourier transform (FRFT) can transform data into the space of the fractional order domain, where fractional order can be used to search for the maximum value of fault. Instantaneous spectrum estimation is an important method to analyze non-stationary signals. Through it, the transient characteristics of these signals can be obtained in both time and frequency domain. A new fault diagnosis method for rolling bearing is proposed by combining instantaneous spectrum estimation with FRFT. Firstly, the optimal order of fractional Fourier transform is determined using the principle of maximum kurtosis coefficient. Then the 2-D fractional domain power spectrum under the selected fractional order is obtained using the rotation property of fractional Fourier transform. Furthermore, the energy intensity of each frequency component in the fractional domain is achieved by integrating the time-frequency spectrum along the time axis, and is applied to the fault diagnosis. The simulated signal and some actual bearing fault data are processed to verify the effectiveness with Renyi entropy introduced as an evaluation parameter. Experimental results show that the new algorithm has higher time-frequency resolution. Especially, there is a good aggregation for weak fault signals. The proposed method can obtain more accurate characteristic frequency identification and provide a new alternative for fault diagnosis of rolling bearing.

Keywords Fault diagnosis · Rolling bearing · Fractional Fourier transform · Instantaneous spectrum

Introduction

Lots of faults about rotating machinery are related to rolling bearings which have a great influence on the working state of the machine [1, 2]. Therefore, study on rolling bearing fault diagnosis is of great significance.

The research on fault diagnosis of rolling bearing began in 1960s. In 1974, Boeing invented the technology of resonance demodulation. Modern analytical methods of fault diagnosis are mainly based on feature extraction in time domain and frequency domain. The time domain analysis of rolling bearing fault needs complex parameter comparison, and the stability and sensitivity are not good. Frequency domain analysis method solves these problems to a certain extent. However, it is not enough to study the complex non-stationary signals separately from the time domain or frequency domain. It is necessary to analyze the signals both in time and frequency domain. Meanwhile mechanical fault signals are non-stationary signals, it is not comprehensive that the characteristics of fault signals are described only in time domain or frequency domain [3].

Scholars hope to analyze the characteristics of fault signals in time and frequency domain simultaneously [4]. Short-time Fourier transform (STFT) is the first one to be used. This method can obtain better local characteristics in time-frequency domain. However, STFT is limited by the selection of window functions and is difficult to analyze various situations [5]. In order to get rid of this limitation, researchers put forward Wavelet technology. Experiments prove that Wavelet method has strong resolving power to the fault signal. Wavelet method is widely used in bearing fault diagnosis because of its multi-scale decomposition [6, 7]. As a priori algorithm, Wavelet analysis needs to set parameters in advance, and the

✉ J-h. Cai
cjh1021cjh@163.com

✉ Y-l. Xiao
xiaoyongliang@hufe.edu.cn

[1] Cooperative Innovation Center for the Construction and Development of Dongting Lake Ecological Economic Zone, Hunan University of Arts and Science, Changde 415000, China

[2] School of Information Technology and Management, Hunan University of Finance and Economics, Changsha 410205, China

improper selection of parameters will have a bad impact on the results [8]. Wigner-Ville method is used in the field of mechanical fault diagnosis due to its high time-frequency resolution and good aggregation. However, the biggest disadvantage of this method is the existence of cross terms [9]. In recent years, some new signal processing methods, such as empirical mode decomposition and auto-encoder, are also used in fault diagnosis [10–12]. Intelligent fault diagnosis of rolling bearing has also been developed based on hierarchical convolutional network, learning machine, and genetic algorithm [13–16].

Fractional Fourier transform is a signal processing technology developed recently. Its remarkable advantage over Fourier transform is that it can provide more choices for time-frequency analysis and obtain some improvements in performance. Almeida laid the foundation for time-domain analysis in fractional domain [17, 18]. Power spectrum, which describes the average power of each frequency component in a random process, is one of the important representations of random signals [19, 20]. Referring to fractional time-frequency rotation characteristics, the power spectrum distribution is directly calculated in fractional domain. Furthermore, the energy intensity of each frequency component in fractional domain is achieved by integrating the time-frequency spectrum along the time axis, which is applied to the fault diagnosis. The proposed algorithm can separate noise signals from the fault signals in the fractional order domain, which provides a good condition for further extracting their time domain and frequency domain characteristics.

Method Principle

Fractional Fourier Transform

The fractional Fourier transform of signal $x(t)$ is defined as following [17, 18].

$$M_\alpha(u) = FRFT_\alpha[x(t)] = \int_{-\infty}^{+\infty} x(t) N_\alpha(t,u)dt \tag{1}$$

Here,

$$N_\alpha(t,u) = \begin{cases} \sqrt{\frac{1-j\cot\alpha}{2\pi}} \exp\left(j\frac{u^2+t^2}{2}\cot\alpha - j\frac{ut}{\sin\alpha}\right) & \alpha \neq n\pi \\ \delta(u-t) & \alpha = 2n\pi \\ \delta(u+t) & \alpha = (2n+1)\pi \end{cases} \tag{2}$$

α is the transform angle and $\alpha < |\alpha| < \pi$. Transform order is $p = 2\alpha/\pi$. When $p = 1$, $FRFT$ is Fourier transform.

Considering the relationship between the one-dimensional power spectrum and the spectrum distribution, the 2D distribution of power spectrum in the fractional domain with angle of α is given [21].

$$PSD_{(u-v,\alpha)}(u,v) = \frac{1}{2T}\left|\int M_\alpha\left(u'\right) H(u'-u) e^{-j2\pi u' v} du'\right|^2 \tag{3}$$

In the Formula, $M_\alpha(u)$ is the result of fractional Fourier transform at α angle, which is applied for a signal with a length T. $H(u)$ is a fractional domain window function. In order to have a higher time-frequency resolution,$H(u)$ is chosen as Gauss window function generally. u' is a variable in the u - v domain. According to 20th reference, the fractional domain power spectrum of α angle is defined as

$$PSD_\alpha(u) = \lim_{T\to\infty} \frac{1}{2T} |M_\alpha(u)|^2 \tag{4}$$

In the formula, $M_\alpha(u)$ is the result of fractional Fourier transform of $x(\tau)$ at α angle based on Eqs. (1) and Eq. (2), where $x(\tau)$ is a segment of signal intercepted from $x(t)$, with a length T.

Time Frequency Distribution of Power Spectrum in Fractional Domain

In order to have a clear physical meaning, the power spectrum is rotated from the u - v plane of the fractional field to the t - f plane. Then the direct expression of the time-frequency distribution in the fractional domain is obtained [22].

$$\begin{aligned} &PSD_{(t-f,a)}(t,f) = R_a\{TFPSD_a(u,v)\} \\ &= R_a\left\{\frac{1}{2T}\left|\int_{-\infty}^{+\infty}\int_{-\infty}^{+\infty} x\left(t'\right) N_a\left(t',u'\right) dt' \times H(u'-u) e^{-j2pu'u} du'\right|^2\right\} \\ &= R_a\left\{\frac{1}{2T}\left|\int_{-\infty}^{+\infty}\int_{-\infty}^{+\infty} x\left(t'\right) e^{jp\left(u^2-v^2\right)sinacosa} \times h(t'-ucosa+vsina) e^{-j2pt'(usina+vsina)} dt'\right|^2\right\} \\ &= \frac{1}{2T}\left|\int_{-\infty}^{+\infty} x\left(t'\right) h(t'-t) e^{-j2pt'f} dt'\right|^2 \end{aligned} \tag{5}$$

$$\begin{pmatrix} t \\ f \end{pmatrix} = R_{-\alpha}\begin{pmatrix} u \\ v \end{pmatrix} = \begin{pmatrix} \cos\alpha & -\sin\alpha \\ \sin\alpha & \cos\alpha \end{pmatrix}\begin{pmatrix} u \\ v \end{pmatrix} \tag{6}$$

In the form, $t'$is a variable in t - f domain. R_α represents rotation and the Formula (5) is the rotation equation.

And $h(t)$ is determined by the fractional Fourier transform of $H(u)$.

$$h(t) = FRFT_P[H(u)] \tag{7}$$

Formula (5) shows that the power spectrum distribution in the fractional domain is identical with the two-dimensional spectrum in form. The key lies in the selection of Gauss window function in fractional domain. According to the conclusions given in document [23, 24], when

$$H(u) = e^{-\frac{\pi u^2 B_{xp}}{T_{xp}}}, \tag{8}$$

the aggregation of the power spectrum in the fractional domain will be optimal.T_{x_p} andB_{x_p} are the time-wide and frequency-wide of signal $x(t)$ in the p order fractional domain.

In the vast literature, there are many ways to determine the best order p. Considering the characteristics of the fault signal, the maximum kurtosis coefficient method is adopted as following [25–27].

$$K\{M_\alpha(u)\} = \frac{E\left[\left(|M_\alpha(u)|-\left|\overline{M}_\alpha(u)\right|\right)^4\right]}{E^2\left[\left(|M_\alpha(u)|-\left|\overline{M}_\alpha(u)\right|\right)^2\right]} \tag{9}$$

$$p = \arg\max_{0\le p<2} K\{M(u)\} \tag{10}$$

In the formula, $\overline{M}_\alpha(u)$ is the mean value of$M_\alpha(u)$and E is mathematical expectation.

Quantitative Evaluation Index

Entropy is a tool to measure the uncertainty of information. For signals with strong randomness, the greater the uncertainty, the greater the entropy. For signals with strong certainty, the entropy is smaller. Applied to the time-frequency analysis, the more concentrated the energy distribution is, the smaller the uncertainty is and the smaller the entropy is. The more dispersed the energy is, the greater the uncertainty is and the larger the entropy is. The entropy value can be used to judge the degree of time-frequency energy convergence, and then judge the result of time-frequency analysis.

Renyi entropy, as evaluation index, is used to evaluate the advantages of the proposed algorithm and other algorithms. Renyi generalized the concept of entropy in 1973, and put forward the Renyi entropy.

$$R_\alpha(p) = \frac{1}{1-\alpha}\log_2\frac{\sum_i p_i^\alpha}{\sum_i p_i} \tag{11}$$

Where, α is the order of entropy, when $\alpha \to 1$, Renyi entropy became Shannon entropy. p_i is the probability density ($i = 1, 2,\ldots$).

Simulation Analysis

In order to verify the effectiveness of the presented algorithm, a set of sinusoidal frequency modulation signals are selected for testing. Its time domain waveform and instantaneous frequency distribution are shown in Fig. 1. According to the theory deduced above, the optimal order p is searched by Eqs. (9) and Eq. (10). Then the optimal window function $H(u)$ in the fractional domain is obtained from Eq. (8). And the u - υ distribution of the power spectrum in the fractional domain can be achieved by Eq. (3). Finally, the t - $f$distribution of the power spectrum in the fractional domain can be obtained based on Eq. (5).

For comparison, the results from STFT method and the improved Wigner-Ville method are given. Figure 2 shows the time-frequency spectrum and the power spectrum of the simulated signal from STFT, the improved Wigner-Ville and the proposed method respectively. Here, the smoothing pseudo Wigner-Ville distribution is used to effectively solve the problem of cross-interference in Wigner-Ville distribution. From Fig. 2(a), it can be seen that the two-dimensional spectrum of STFT exhibits the instantaneous frequency characteristics of the simulated signal with sinusoidal variation. However, the resolution of the two-dimensional spectrum is low, and the bright band which represents the frequency change is very wide. In Fig. 2(b), the obtained marginal spectrum (power spectrum) is also smooth and lacks peak information. In the improved Wigner-Ville spectrum shown in Fig. 2(c), the clarity and resolution are improved. Its marginal spectrum in Fig. 2(c) is more detailed than that shown in Fig. 2(b), but its practicability is still low. The time-frequency spectrum and power spectrum of the fractional domain obtained from the presented method are shown in Fig. 2(e) and (f). In the 0.05–0.1 Hz frequency band, the amplitude variation of each frequency component is shown in Fig. 2(f) clearly while the variation is smoothed in Fig. 2(b) and (d).

Renyi entropy of time-frequency spectrum from three methods are compared in Table 1. Compared with the STFT method, the entropy value has been reduced from 9.9979 to 7.9664 using the proposed method. And it is smaller than that of the smoothing pseudo Wigner-Ville method. The time-frequency aggregation of the instantaneous spectrum from FRFT is greatly enhanced. It can be seen that the accuracy of instantaneous energy distribution and marginal spectrum has been greatly improved. Resolution is significantly higher than that of Fig. 2(a) and (c). The bright band with sinusoidal shape is more concentrated, the time frequency clustering is greatly improved and the brightness is uniform. The time-frequency distribution of energy coincides well with the instantaneous frequency distribution shown in Fig. 1. The marginal spectrum is no longer smooth, and the peak information is displayed, which is conducive to further identification.

Measured Data Processing

To further illustrate the effectiveness of the proposed method, it is applied to fault diagnosis of rolling bearings. The experimental data come from the electrical engineering laboratory of Case Western Reserve University, USA. The tested bearing is 6205-2RS JEM SKF. The parameters of some main components are described below: Rolling element number is 9, the contact angle is 0, bearing speed is 1750 r/min. Inner diameter is 25.0012 mm, outer diameter is 51.9989 mm, thickness is

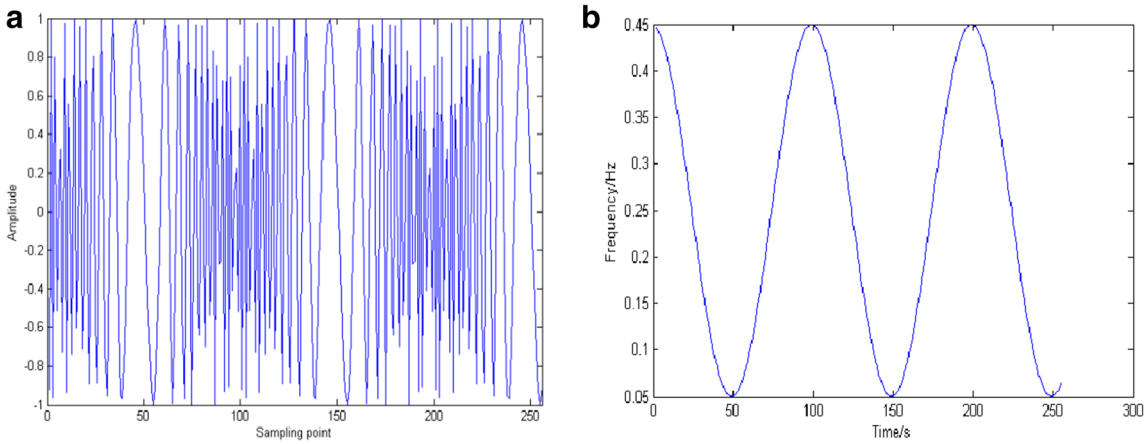

Fig. 1 Time domain waveform of sinusoidal frequency modulation signal (**a**) and it Instantaneous frequency distribution (**b**)

14.5906 mm, pitch diameter is 39.0398 mm, rolling body diameter is 7.9412 mm. In outer ring, damage diameter is 0.1778 mm which is made by the electric spark machining. The sampling frequency of vibration signal is 12 kHz. The selected data contains fault signals from the inner, outer and rolling rings and its time series are shown in Fig. 3. Based on the theory, the fault frequency of bearing can be calculated as following [2]:

Fault frequency on inner race:

$$f_i = \frac{z}{2}\left(1 + \frac{d}{D}\cos\alpha\right) f_r \tag{12}$$

Fault frequency on outer race:

$$f_o = \frac{z}{2}\left(1 - \frac{d}{D}\cos\alpha\right) f_r \tag{13}$$

Fault frequency on rolling ball:

$$f_b = \frac{D}{d}\left(1 - \left(\frac{d}{D}\right)^2 \cos^2\alpha\right) f_r \tag{14}$$

Here, f_r is the bearing speed, z is the number of balls, d is the rolling diameter, D is the bearing pitch diameter, α is rolling contact angle. So based on the theoretical formula, fault frequency can be determined as: $f_i \approx 158$ Hz, $f_o \approx 104$ Hz, $f_b \approx 137$ Hz.

Firstly, the vibration signal of rolling bearing with outer ring fault is considered. The smoothing pseudo Wigner-Ville spectrum and its corresponding marginal spectrum of outer ring fault signal are shown in Fig. 4(a) and (b). In time-frequency spectrum, there is an obvious bright band near 104 Hz, but it is discontinuous and its divergence is large. In the marginal

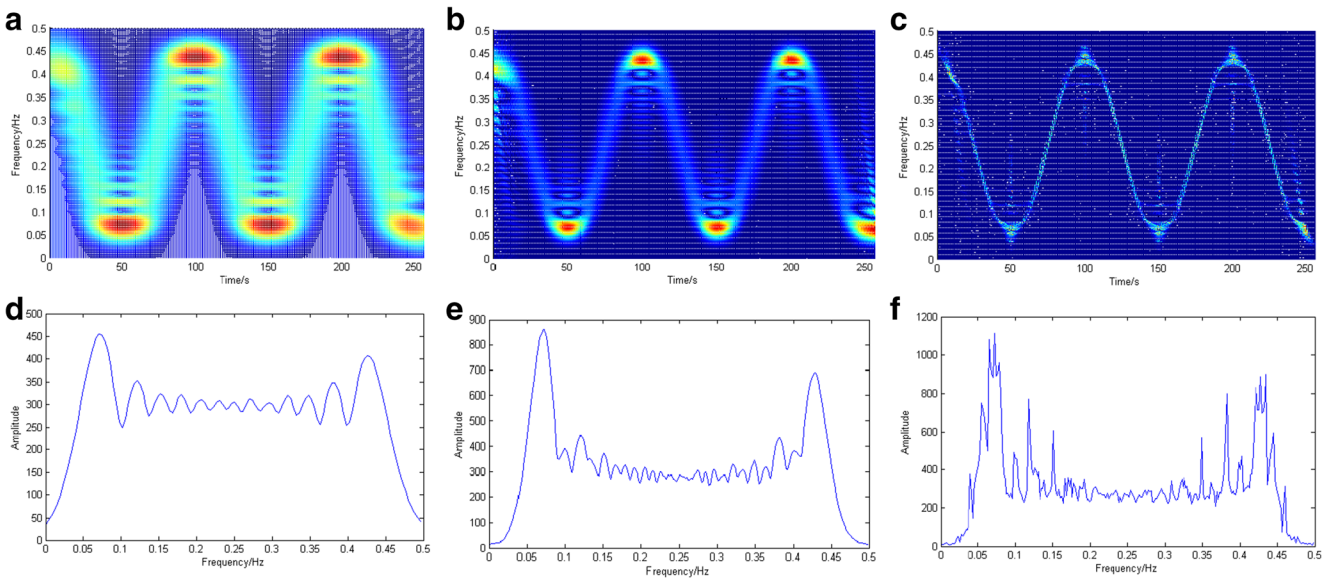

Fig. 2 Time-frequency spectrum and power spectrum of simulated signal: (**a**), (**b**) is from STFT; (**c**), (**d**) is from the smoothing pseudo Wigner-Ville method and (**e**), (**f**) is from the presented method

Table 1 Comparison of Renyi entropy of time-frequency spectrum from three methods

Evaluation indexe	Method		
	STFT method	The smoothing pseudo Wigner-Ville method	The presented method
Renyi entropy	9.9979	9.0173	7.9664

spectrum, there is an obvious spectral peak at the characteristic frequency point 104 Hz, and the amplitude is very large. This is because the fault position acts as an excitation source when the outer ring of the rolling bearing fails, and the excitation produces an impact every rotation. The vibration signal of the impact is expressed by the modulation of the amplitude modulation signal to the carrier signal of the bearing natural frequency, where the modulation frequency is the fault characteristic frequency. Therefore, the bearing fault lists in outer ring, which can be obtained from the spectrum line at the characteristic frequency f_o = 104 Hz. However, through careful observation it can be shown that other components of the fault diagnosis interference are greater and other harmonic components can't be shown in the smoothing pseudo Wigner-Ville spectrum and its corresponding marginal spectrum.

The time-frequency spectrum and the corresponding marginal spectrum in the fractional domain are shown in Fig. 4(c) and d. In the time-frequency spectrum, not only the 104 Hz energy band is brighter and more concentrated, but also the second harmonic can be seen. In the marginal spectrum, the characteristic frequency of 104 Hz, its harmonics 208 Hz and 312 Hz all can be marked clearly, which is more helpful to the diagnosis of bearing fault. Obviously, the proposed method can get more detailed time-frequency spectrum and higher time-frequency resolution. The Renyi entropy of time-frequency spectrum of the measured data are shown in Table 2. Compared with the smoothing pseudo Wigner-Ville method, the entropy value has been reduced from 8.998 to 7.8468 by using the proposed method. The energy distribution is more concentrated. The time-frequency accumulation spectrum of the fractional energy band has the characteristics of focusing. The fractional energy band can highlight the target component to the greatest extent, and restrain other components and noise. This feature is especially suitable for extracting weak fault characteristics of vibration signals.

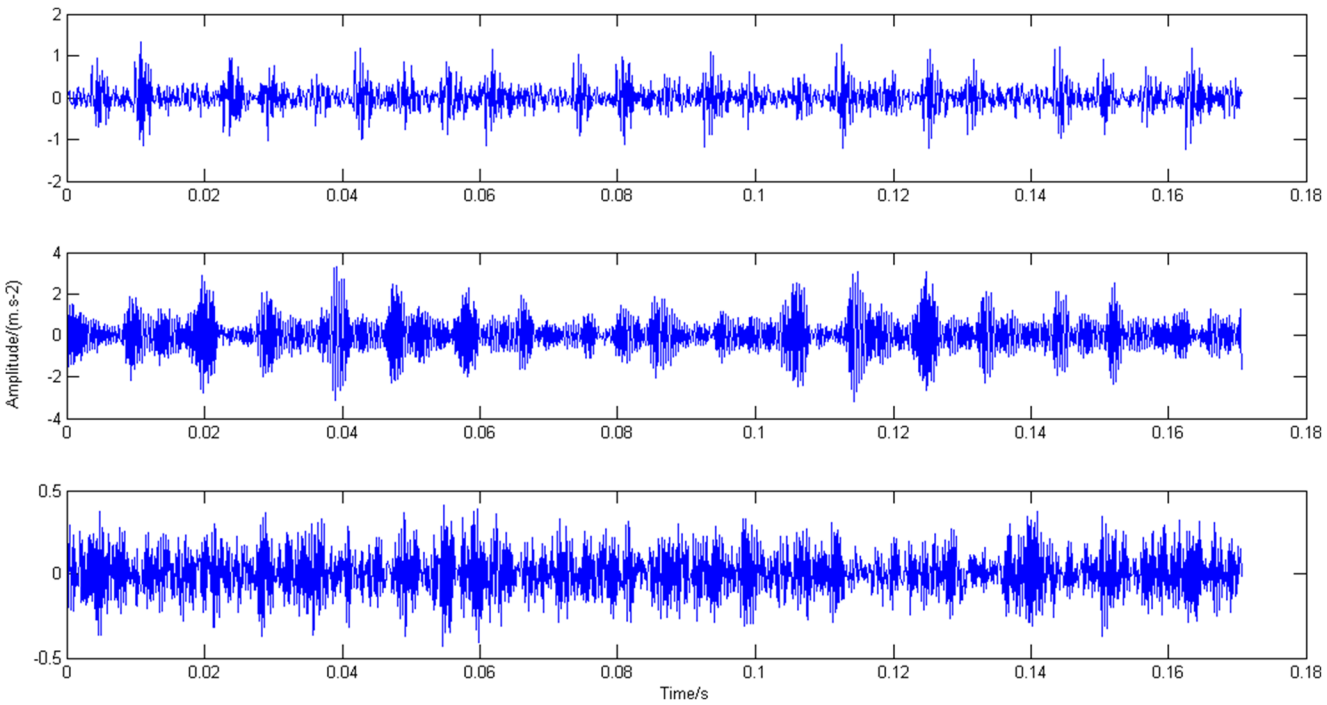

Fig. 3 Measured rolling bearing fault signal: (**a**) inner ring, outer ring (**b**) and the roller(**c**)

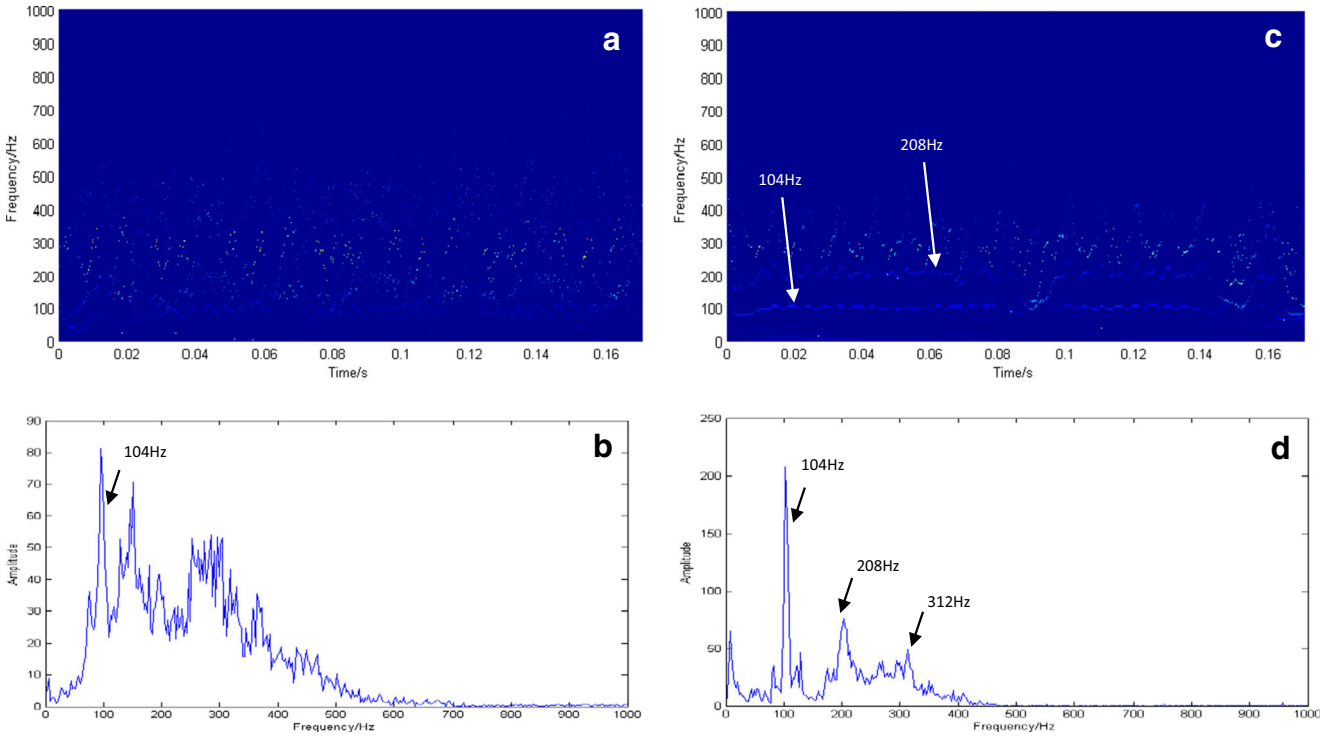

Fig. 4 Time-frequency spectrum and power spectrum of outer race fault signal: (**a**), (**b**) based on the smoothing pseudo Wigner-Ville method; (**c**), (**d**) based on the proposed method

Furthermore, the rolling bearing vibration signals from inner ring and rolling body are analyzed. Similarly, the results are compared with the smoothing pseudo Wigner-Ville method. According to the physical information of rolling bearing, we can calculate the fault frequency of ring as: $f_i = 158$ Hz and $f_b = 137$ Hz. Figures 5 and 6 show the processed results. It can be seen that the conclusions obtained from the analysis are consistent with these shown in Fig. 4. Similarly, these Renyi entropy values listed in Table 2 reflect the same conclusion that the proposed algorithm has higher time-frequency resolution than smoothing pseudo Wigner-Ville method. In the fractional domain time-frequency spectrum and the corresponding marginal spectrum, the characteristic frequency and its harmonics can be marked more clearly. It is more conducive to the diagnosis of bearing failure. The presented method is better than the smoothing pseudo Wigner-Ville method in fault diagnosis.

Conclusion

In this paper, a new fault diagnosis method is proposed based on instantaneous power spectrum estimation in fractional domain. Here, the maximum kurtosis coefficient method is used to estimate the spectrum of optimal fractional domain. And the power spectrum distribution in fractional domain is transformed into time-frequency distribution by using fractional domain time-frequency analysis technique. This method enables intuitive physical meaning in fractional domain of the power spectrum distribution. At the same time, the resolution of two-dimensional power spectrum is improved. Especially in weak signal analysis, there is a good aggregation for weak fault signals. Experimental results of simulation signal and real data show that the proposed algorithm has higher time-frequency resolution than the smoothing pseudo Wigner-Ville method, and can obtain

Table 2 Renyi entropy of time-frequency spectrum of the measured data

Bearing fault signal	Method	
	The smoothing pseudo Wigner-Ville method	The presented method
inner ring	8.9426	7.8593
outer ring	8.9981	7.9686
the roller	8.7747	7.5986

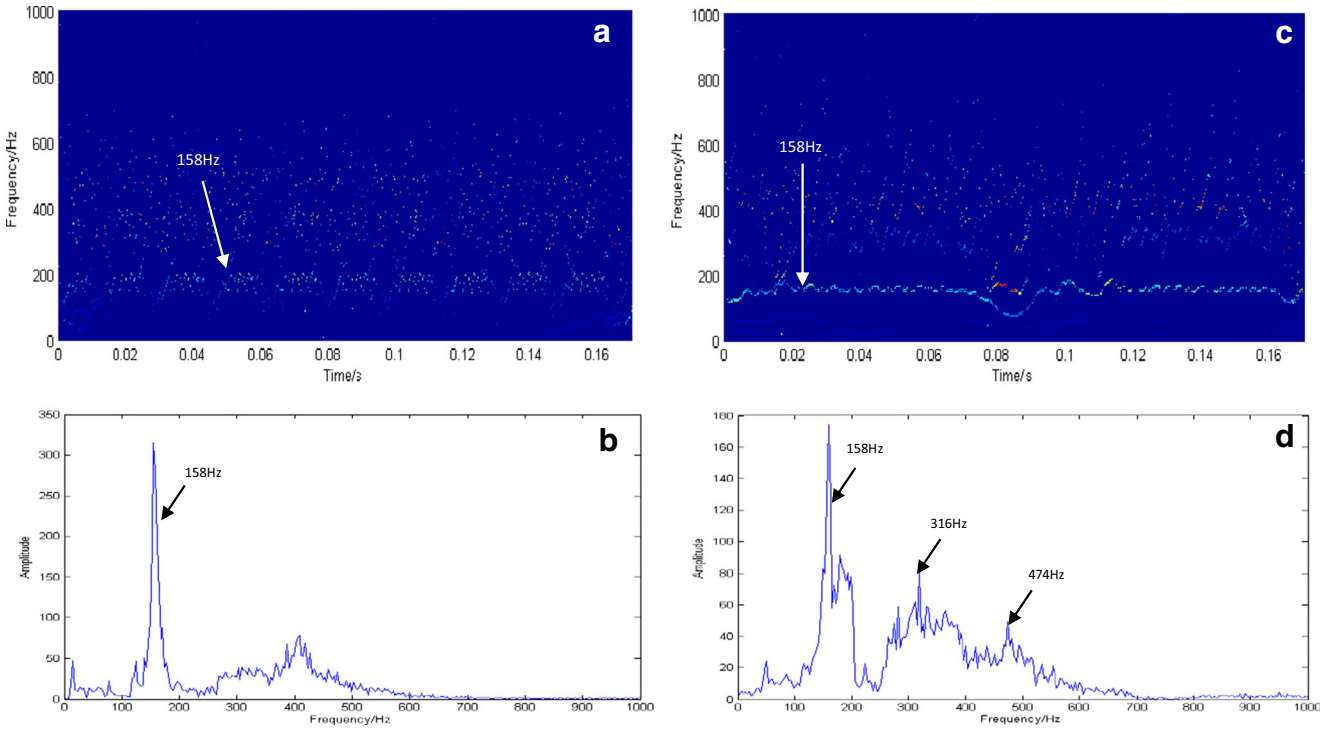

Fig. 5 Time-frequency spectrum and power spectrum of inner race fault signal: (**a**), (**b**) based on the smoothing pseudo Wigner-Ville method; (**c**), (**d**) based on the proposed method

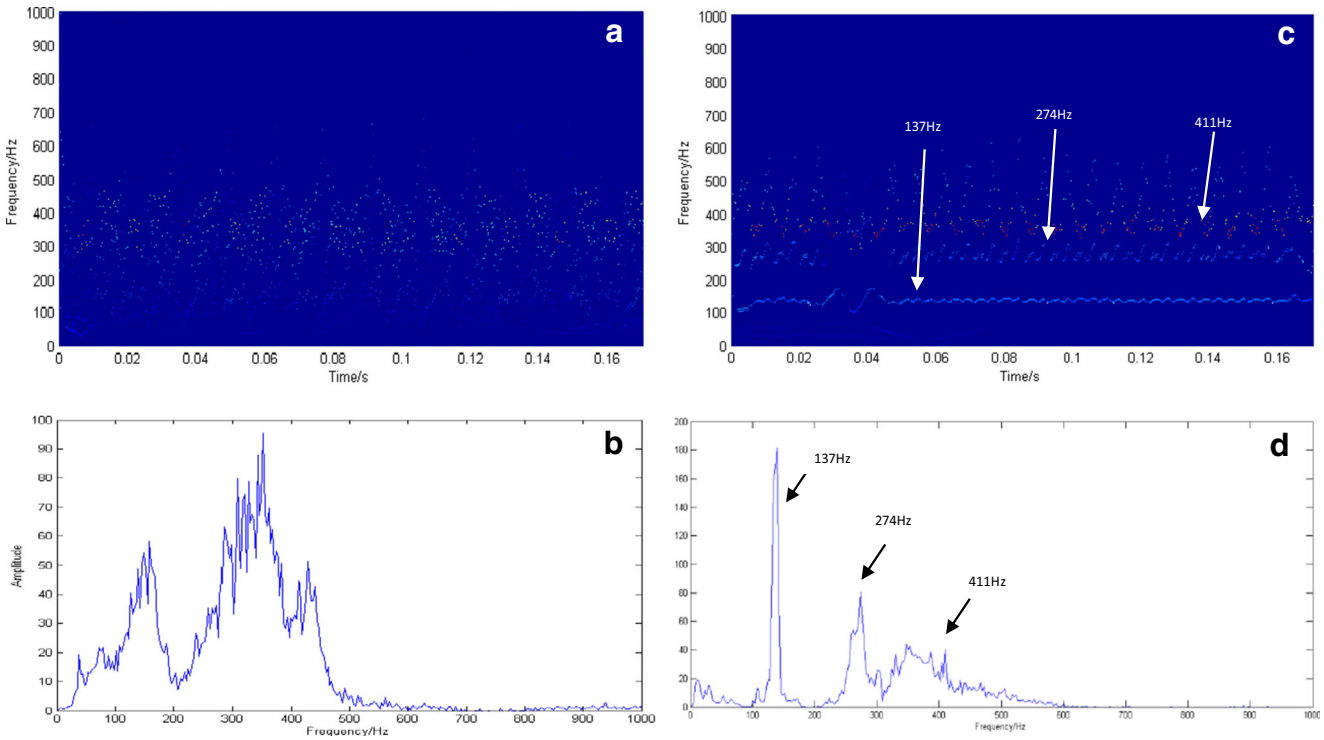

Fig. 6 Time-frequency spectrum and power spectrum of rolling body fault signal: (**a**), (**b**) based on the smoothing pseudo Wigner-Ville method; (**c**), (**d**) based on the proposed method

more accurate characteristic frequency identification for fault diagnosis.

Acknowledgments The author(s) disclosed receipt of the following financial support for the research, authorship, and/or publication of this article: The authors express their appreciation for the financial support provided by the National Natural Science Foundation of China (project no: 41304098), Hunan Province Applied Characteristic Subject "Electronic Science and Technology" and the Natural Science Foundation of Hunan (project no: 2017JJ2192, 2017JJ2015), Hunan Province Key Laboratory of Photoelectric Information Integration and Optical Manufacturing Technology.

Declarations

Conflict of Interest On behalf of all authors, the corresponding author states that there is no conflict of interest.

References

1. Serhat S, Emine A (2003) Feature extraction related to bearing damage in electric motors by wavelet analysis. J Frankl Inst 340(2):125–134
2. Cai JH (2015) Fault diagnosis of rolling bearing based on empirical mode decomposition and higher order statistics. Proc IMechE Part C:J Mech Eng Sci 229(9):1630–1638
3. Sun LY, Qu D, Tian T (2005) Application of Fourier transform and wavelet transform to signal fault diagnosis. J Liaoning Inst Technol 25(3):155–158
4. Wang S, Cai G, Zhu Z (2015) Transient signal analysis based on Leven berg-Marquardt method for fault feature extraction of rotating machines. Mech Syst Signal Process s54-55(3):16–40
5. Durak L, Arikan O (2003) Short time Fourier transform: two fundamental properties and an optimal implementation. IEEE Transform Signal Process 51(5):1231–1242
6. Acharya UR, Yanti R, Swapna G, Sree VS, Martis RJ, Suri JS (2013) Automated diagnosis of epileptic electroencephalogram using independent component analysis and discrete wavelet transform for different electroencephalogram durations. Proc Inst Mech Eng Part H 227:234–244
7. Jong-Hyo A, Dae-Ho K, Bong-Hwan K (2014) Fault detection of a roller-bearing system through the EMD of a wavelet De-noised signal. Sensors 14(8):15022–15038
8. Lin J, Qu LS (2003) Feature extraction based on Morlet wavelet and its application for mechanical fault diagnosis. J Sound Vib 234(1):135–148
9. Khan NA, Taj IA, Jaffri MN (2011) Cross-term elimination in Wigner distribution based on 2D signal processing techniques. Signal Process 91(3):590–599
10. Xiang JW, Zhong YT (2017) A fault detection strategy using the enhancement ensemble empirical mode decomposition and random decrement technique. Microelectron Reliab 75:317–326
11. Meng Z, Zhan XY, Li J, Pan ZZ (2018) An enhancement denoising autoencoder for rolling bearing fault diagnosis. *Meas* 130:448–454
12. He ZY, Cheng JS, Li J, Yang Y (2019) Linear maximum margin tensor classification based on flexible convex hulls for fault diagnosis of rolling bearings. Knowl-Based Syst 173:62–73
13. Lu C, Wang ZY, Zhou B (2017) Intelligent fault diagnosis of rolling bearing using hierarchical convolutional network based health state classification. Adv Eng Inform 32(4):139–151
14. Shao HD, Jiang HK, Li XQ, Wu SP (2018) Intelligent fault diagnosis of rolling bearing using deep wavelet auto-encoder with extreme learning machine. Knowl-Based Syst 140(15):1–14
15. Liu H, Zhou JZ, Zheng Y, Jiang W, Zhang YC (2018) Fault diagnosis of rolling bearings with recurrent neural network-based autoencoders. ISA Trans 77(7):167–178
16. Unal M, Onat M, Demetgul M, Kucukc H (2014) Fault diagnosis of rolling bearings using a genetic algorithm optimized neural network. *Meas* (12):58, 187–196
17. Kamalakkannan R, Roopkumar R (2020) Multidimensional fractional Fourier transform and generalized fractional convolution. Integral Transform Spec Funct 31(2):152–165
18. Almeida LB (1997) Product and convolution theorems for the fractional Fourier transform. IEEE Signal Process Lett 4(1):15–17
19. Elgamel SA, Soraghan JJ (2011) Using EMD-FrFT filtering to mitigate very high power interference in chirp tracking radars. IEEE Signal Process Lett 18(4):263–266
20. Tao R, Zhang F, Wang Y (2008) Fractional power spectrum. IEEE Trans Signal Process 56(9):4199–4206
21. Wang Q, Pepin M, Beach RJ et al (2012) SAR-based vibration estimation using the discrete fractional Fourier transform. Geo-Sci Remote Sens IEEE Trans 50(10):4145–4156
22. Ran T, Siyong Z, Yue W (2002) Adaptive time-varying filter for linear FM signal in fractional Fourier domain. 6th IEEE Int Conf Signal Process 2:1425–1428
23. Holweger W (2012) Frank Walther, Jörg loos, Marcus wolf, Jürgen Schreiber, Werner Dreher, Norbert Kern, Steffen Lutz, non-destructive subsurface damage monitoring in bearings failure mode using fractal dimension analysis. Ind Lubr Tribol 64(3):132–137
24. He X, Ma J (2020) Weak fault diagnosis of rolling bearing based on FRFT and DBN. Syst Scie Control Eng 8(1):57–66
25. Tian L, Peng Z (2014) Determining the optimal order of fractional Gabor transform based on kurtosis maximization and its application. J Appl Geophys 108(9):152–158
26. Jahagirdar AC, Gupta KK (2020) Fractional envelope to enhance spectral features of rolling element bearing faults. J Mech Sci Technol 34(2):573–579
27. Pan Z, Fan H, Zhang Z (2020) Nonuniformly-rotating ship refocusing in SAR imagery based on the bilinear extended fractional Fourier transform. Sensors 20(2):1–13